



# Climatic and hydrologic variability during the past millennium in the eastern Rocky Mountains and northern Great Plains of western Canada

Thomas W.D. Edwards <sup>a,\*</sup>, S. Jean Birks <sup>b</sup>, Brian H. Luckman <sup>c</sup>, Glen M. MacDonald <sup>d</sup>

<sup>a</sup> *Earth and Environmental Sciences, University of Waterloo, Waterloo, Canada ON N2L 3G1*

<sup>b</sup> *Alberta Research Council, 3608 - 33 Street NW, Calgary, Canada AB T2L 2A6*

<sup>c</sup> *Geography, University of Western Ontario, London, Canada ON N6A 5C2*

<sup>d</sup> *Geography, University of California, Los Angeles, CA 90095-1524, USA*

Received 12 June 2007

## Abstract

Modelling of tree-ring  $\delta^{13}\text{C}$  and  $\delta^{18}\text{O}$  data from the Columbia Icefield area in the eastern Rocky Mountains of western Canada provides fuller understanding of climatic and hydrologic variability over the past 1000 yr in this region, based on reconstruction of changes in growth season atmospheric relative humidity ( $RH_{\text{grs}}$ ), winter temperature ( $T_{\text{win}}$ ) and the precipitation  $\delta^{18}\text{O}-T_{\text{win}}$  relation. The Little Ice Age (~AD 1530s–1890s) is marked by low  $RH_{\text{grs}}$  and  $T_{\text{win}}$  and a  $\delta^{18}\text{O}-T_{\text{win}}$  relation offset from that of the present, reflecting enhanced meridional circulation and persistent influence of Arctic air masses. Independent proxy hydrologic evidence suggests that snowmelt sustained relatively abundant streamflow at this time in rivers draining the eastern Rockies. In contrast, the early millennium was marked by higher  $RH_{\text{grs}}$  and  $T_{\text{win}}$  and a  $\delta^{18}\text{O}-T_{\text{win}}$  relation like that of the 20th century, consistent with pervasive influence of Pacific air masses because of strong zonal circulation. Especially mild conditions prevailed during the “Medieval Climate Anomaly” ~AD 1100–1250, corresponding with evidence for reduced discharge in rivers draining the eastern Rockies and extensive hydrological drought in neighbouring western USA.

© 2008 Published by University of Washington.

**Keywords:** Carbon isotopes; Oxygen isotopes; Dendroclimatology; Hydrological drought

## Introduction

Tree-ring-based investigations have generated increasingly detailed understanding of climatic and hydrologic variability over the past 1000 yr in western North America. Much of this research has focused on reconstructing changes in temperature, precipitation, streamflow and glacier mass balance over the last few centuries (e.g., Luckman, 2000; Watson and Luckman, 2001, 2004, 2005, 2006) and mapping variability in drought frequency and severity over varying time-scales (e.g., Meko et al., 2001; Cook et al., 2004, 2007; Herweijer et al., 2006; MacDonald et al., 2007, 2008). However, the development of more comprehensive understanding of climate history over the past millennium has been hampered by the relative paucity of long tree-ring chronologies, especially those spanning the early

millennium, prior to ~AD 1500 (D'Arrigo et al., 2006), as well as by controversy over the ability of traditional tree-ring-based methods to reconstruct low-frequency climate signals (Mann et al., 1999, 2005; Esper et al., 2002, 2005a,b; von Storch et al., 2004).

Recent advances in the documentation of climatic and hydrologic variability specific to western Canada (Fig. 1) include a ringwidth-based reconstruction of streamflow in the North Saskatchewan River (Case and MacDonald, 2003), which rises in the Columbia Icefield area of the eastern Rocky Mountains and ultimately drains eastward to Hudson Bay, and a newly revised and verified reconstruction of summer maximum temperature at upper alpine treeline within the Columbia Icefield area based on maximum latewood density and ringwidth (Luckman and Wilson, 2005). Both of these records span the full last millennium. Here we add new 1000-yr reconstructions of changes in winter temperature, growth-season relative humidity and the precipitation  $\delta^{18}\text{O}$ -temperature relation

\* Corresponding author. Fax: +1 519 746 7484.

E-mail address: [twdedwar@uwaterloo.ca](mailto:twdedwar@uwaterloo.ca) (T.W.D. Edwards).

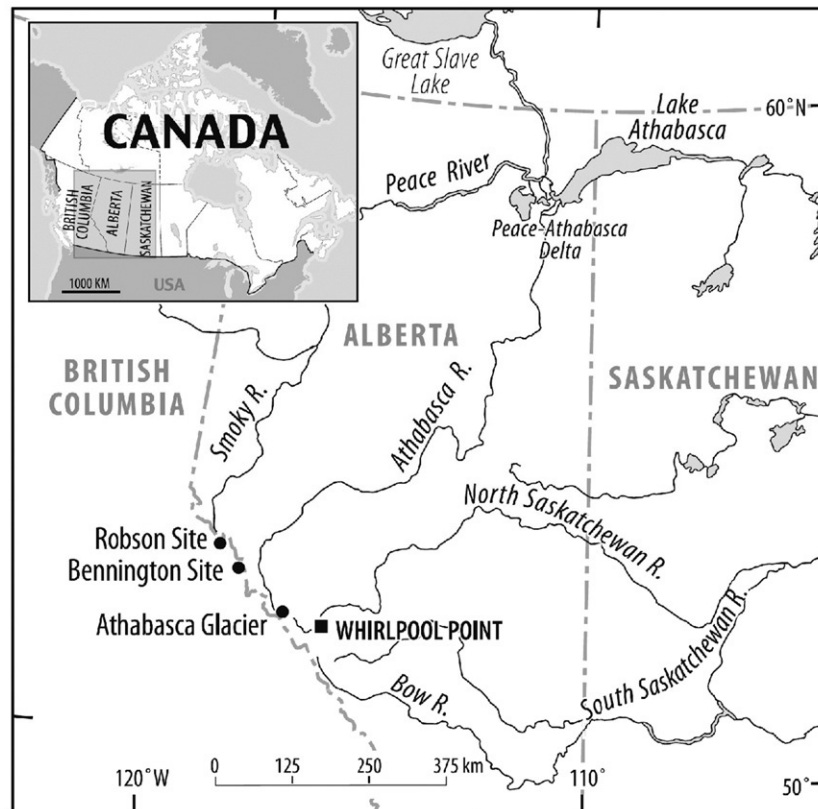


Figure 1. The Columbia Icefield area in the eastern Rocky Mountains of western Canada includes the headwaters of the Athabasca River and the Smoky River (a tributary of the Peace River), which form the southernmost reaches of the Mackenzie River system, and the North Saskatchewan River, a major tributary of the Saskatchewan River system. The Peace-Athabasca Delta is located at the west end of Lake Athabasca. Tree-ring isotope chronologies illustrated in Figure 2 originated from subfossil and living material collected near the Athabasca Glacier, an outlet glacier of the Columbia Icefield, and the nearby Bennington and Robson glaciers. The North Saskatchewan River streamflow reconstruction of Case and MacDonald (2003) shown in Figure 5 is based on trees sampled at Whirlpool Point.

derived from modelling of tree-ring stable-isotope data from the same area. This suite of records allows us to probe key features of climatic and hydrologic change over the past millennium. We focus in particular on better characterization of conditions during medieval times and the subsequent transition into the Little Ice Age. Intriguing new discoveries include evidence of previously unrecognized winter warmth during the Medieval Climate Anomaly (~AD 1100–1250) and shifts in the inferred precipitation  $\delta^{18}\text{O}$ –temperature relation that define the LIA (~AD 1530s–1890s) as a remarkably discrete local climate episode.

## Background

Holocene climate variability over millennial timescales reflects fluctuations in the strength and pattern of global atmospheric circulation (Lamb, 1977; Kreutz et al., 1997; Folland et al., 2001), with well-documented effects on terrestrial environments (e.g., Bryson and Wendland, 1967; Bartlein et al., 1984; MacDonald et al., 2000; Hammarlund et al., 2004). In some instances evidence also exists for associated fluctuations in the relation between the isotopic composition of precipitation and temperature (Dansgaard, 1964), which is commonly used as a paleotemperature transfer function at mid- and high latitudes (Fricke and O’Neil, 1999). Such circulation-dependent deviations from the modern “Dansgaard” relation have been detected

at various times in North and South America (Yapp and Epstein, 1977; Plummer, 1993; Amundsen et al., 1996; Edwards et al., 1996; Kirby et al., 2001; Ramirez et al., 2003; Fisher et al., 2004), eastern Mediterranean (Lipp et al., 1996), western Europe (McKenzie and Hollander, 1993), Greenland (Hoffmann et al., 2001), Scandinavia (Hammarlund et al., 2002) and elsewhere as an intrinsic component of climate variability and change.

Systematic climate variability over the past millennium in the Northern Hemisphere extratropics is also known from numerous sources, ranging from ice-core glaciochemical records in Greenland (Kreutz et al., 1997) to a variety of high- and low-resolution proxy climate reconstructions from pollen, sediments, tree rings, historical data and other archives in northern Eurasia and North America (e.g., Crowley and Lowery, 2000; Esper et al., 2002; Moberg et al., 2005). Although the spatial pattern of variability is less coherent than that associated with directional change over the past ~150 yr, Northern Hemisphere climate is believed to have fluctuated from being generally mild on average in the early millennium (the classic Medieval Warm Period) to being cool and variable during the subsequent Little Ice Age, followed by recent warming (Bradley et al., 2003; D’Arrigo et al., 2006). Kreutz et al. (1997) concluded that this systematic oscillation reflected a characteristic mode of low-frequency variability in the intensity of meridional atmospheric

circulation, with Little Ice Age cooling attributable to enhanced southward penetration of Arctic air masses in many parts of the Northern Hemisphere. Independent tree-ring-based reconstructions showing persistently negative North Atlantic Oscillation (NAO) index (Cook, 2004) and weakened Pacific Decadal Oscillation (PDO) variability (MacDonald and Case, 2005) during the LIA support this notion.

### Isotope dendrochronology development and modelling

Our approach employs a coupled isotope response–surface model to resolve multi-dimensional patterns of climate variability using carbon- and water-isotope time series developed from tree-ring cellulose. The cellulose  $\delta^{13}\text{C}$  dendrochronology was developed from cross-dated 10-yr increments of 16 sub-fossil snags and living-tree ring sequences of *Picea engelmannii* (Engelmann spruce) from upper alpine treeline sites near Athabasca Glacier (~2000 m asl) and subfossil material from the forefield of Robson Glacier (~1700 m asl) plus living and snag material of *Pinus albicaulis* (whitebark pine) adjacent to Bennington Glacier (~2000 m asl), spanning AD 951–1990 (Fig. 2). Trees in such settings are commonly well-supplied by soil moisture derived from seasonal snowmelt, as verified by their temperature-sensitive ringwidth response, as well as by cellulose oxygen and hydrogen isotope evidence (Clague et al., 1992; Treydte et al., 2006).

Cellulose was purified from finely milled wood samples by sequentially eliminating non-cellulose components using solvent extraction, delignification and alkaline hydrolysis (Sternberg, 1989). The carbon-isotope results reported here extend preliminary data reported by Edwards and Luckman (1996) based on off-line closed-tube combustion of individual decadal increments from 2–5 radii of each tree followed by  $^{13}\text{C}/^{12}\text{C}$  analysis on  $\text{CO}_2$  gas by dual-inlet isotope ratio mass spectro-

metry. The composite  $\delta^{13}\text{C}$  record incorporates 698 analyses in total (one or more per cellulose sample), developed by averaging of decadal increments from individual trees, based on averages of results from multiple radii of the same trees. The raw data revealed strong common low-frequency trends among trees from the three sites, with no apparent systematic differences between sites or species. This coherence is consistent with observations that  $\delta^{13}\text{C}$  data from spruce and pine are essentially interchangeable (Leavitt et al., 2006) and suggests that the composited time series provides a representative record for the Columbia Icefield area. The results are reported as  $\delta^{13}\text{C}$  values in per mil (‰) versus VPDB (Vienna Pee Dee Belemnite) such that  $\delta^{13}\text{C} = 1000((R_{\text{sample}}/R_{\text{VPDB}}) - 1)$ , where  $R$  is the  $^{13}\text{C}/^{12}\text{C}$  ratio, following correction for the effect of fossil fuel combustion since AD 1850 (“Suess effect”) on the  $^{13}\text{C}/^{12}\text{C}$  ratio of atmospheric  $\text{CO}_2$  (see Table 1 in McCarroll and Loader, 2004). Average reproducibility of analyses on individual samples was better than  $\pm 0.2\%$ .

The oxygen-isotope record is based on 935 individual analyses (minimum of two per cellulose sample) of decadal increments from 2–4 radii each from a 12-tree subset spanning AD 951–1990 using an elemental analyser interfaced to a continuous-flow isotope ratio mass spectrometer, measuring  $^{18}\text{O}/^{16}\text{O}$  ratio on  $\text{CO}$  gas. Results are reported as  $\delta^{18}\text{O}$  values in per mil (‰) such that  $\delta^{18}\text{O} = 1000((R_{\text{sample}}/R_{\text{VSMOW}}) - 1)$ , where  $R$  is the  $^{18}\text{O}/^{16}\text{O}$  ratio in sample and VSMOW (Vienna Standard Mean Ocean Water), standardized to  $\delta^{18}\text{O}_{\text{SLAP}} = -55.5\%$  (Coplen, 1996). Reproducibility of analyses on individual samples was better than  $\pm 0.3\%$ . The  $\delta^{18}\text{O}$  record was developed by averaging of decadal increment data from radii and trees, as for the  $\delta^{13}\text{C}$  time series. Although a higher level of scatter is apparent than for  $\delta^{13}\text{C}$  (in part attributable to shallower sample depth and slightly larger analytical uncertainties), the two species again appear to record common  $\delta^{18}\text{O}$  information, as also concluded by Leavitt et al.

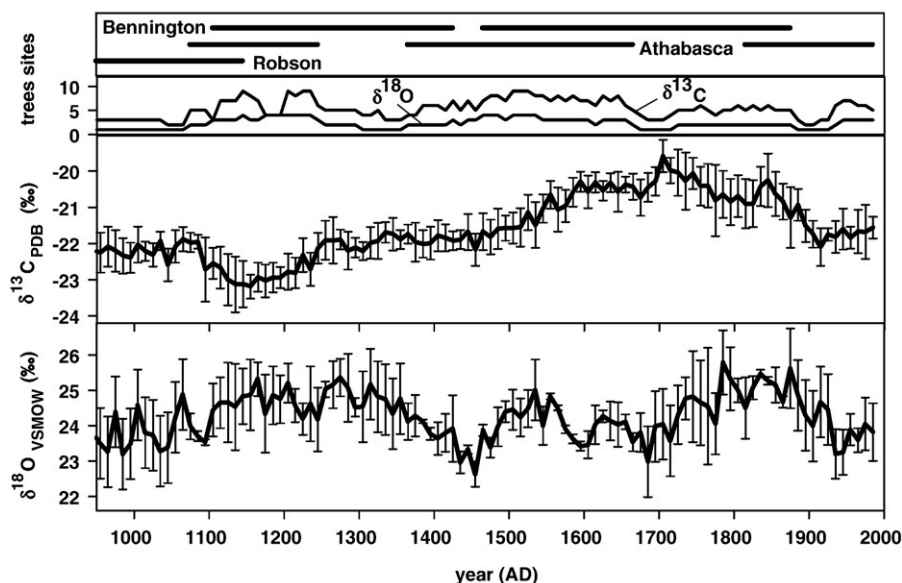


Figure 2. Decadal cellulose  $\delta^{13}\text{C}$  and  $\delta^{18}\text{O}$  dendrochronologies based on subsampling of selected living and subfossil snags of *Picea engelmannii* from the Athabasca and Robson sites and subfossil snags of *Pinus albicaulis* collected from the Bennington site. The two upper panels indicate the intervals spanned by trees from each site and the respective sample depths for the two isotope dendrochronologies.

(2006). Error bars in Figure 2 indicate one standard deviation for decades spanned by multiple trees (mean  $\pm 0.46$  ‰ for  $\delta^{13}\text{C}$  and  $\pm 0.55$  ‰ for  $\delta^{18}\text{O}$ ), with  $\pm 1$  ‰ used as a default uncertainty for  $\delta^{18}\text{O}$  values in four intervals spanned by single trees (AD 951–1060, 1301–1359, 1671–1720, 1881–1930).

Our modelling approach is an evolution of the method used by Yakir et al. (1994) and Lipp et al. (1996) to probe changes in relative humidity, temperature and the isotopic composition of precipitation since the Roman period at the fortress of Masada, Israel; from  $\delta^{13}\text{C}$  and  $\delta^{18}\text{O}$  of ancient and modern tamarisk wood cellulose; and by Edwards et al. (2000) to examine patterns of climate variability over the past millennium in the Black Forest, Germany, from latewood cellulose  $\delta^{13}\text{C}$  and  $\delta^2\text{H}$  of fir. Other studies combining terrestrial plant cellulose carbon- and water-isotope data include use of  $\delta^{13}\text{C}$  and  $\delta^2\text{H}$  from piñon pine needles for evaluating climate change in southwest USA (Pendall et al., 1999), while  $\delta^{13}\text{C}$  and  $\delta^{18}\text{O}$  data have been coupled in various applications, for example to reconstruct precipitation  $\delta^{18}\text{O}$  from oak in France (Danis et al., 2006), to explore carbon and water dynamics in subalpine plants in Italy and Austria (Scheidegger et al., 2000) and to examine annual cyclicity in mangrove wood (Verheyden et al., 2004).

Here we couple the carbon-isotope response surface calibrated for fir by Edwards et al. (2000) with a simplified oxygen-isotope response surface (e.g., see Edwards and Fritz, 1986; Buhay and Edwards, 1995) modified to incorporate temperature-dependent variability in the  $\delta^{18}\text{O}$  of source water. The carbon-isotope response surface is described by

$$\Delta^{13}\text{C}_{\text{cell}} = (-0.17)\Delta RH_{\text{grs}} + (-0.15)\Delta T_{\text{grs}}, \quad (1)$$

where  $\Delta^{13}\text{C}_{\text{cell}}$  is the  $\delta^{13}\text{C}$  record normalized to the mean of the AD 1941–1990 period (youngest five decadal samples) and  $\Delta RH_{\text{grs}}$  and  $\Delta T_{\text{grs}}$  represent changing daytime atmospheric relative humidity (%) and temperature (K) during the growing season. Equation (1) is consistent with the first-order effect that changing relative humidity exerts on carbon-isotope labelling of plant tissues through variations in stomatal conductance (Farquhar et al., 1982) in company with second-order temperature-dependent influence on photosynthetic activity (Scheidegger et al., 2000; Verheyden et al., 2004). Indeed, as apparent from inspection and consistent with the observations of Lipp et al. (1996) and the analyses of Edwards et al. (2000) and Mayr et al. (2004), Eq. (1) indicates that  $\Delta RH_{\text{grs}}$  should normally exert strongly predominant control on cellulose  $\delta^{13}\text{C}$  under natural environmental conditions, since variations in relative humidity (in %) are commonly an order of magnitude greater than variations in temperature (in K).

The analogous oxygen-isotope response surface is described by

$$\Delta^{18}\text{O}_{\text{cell}} = (-0.28)\Delta RH_{\text{grs}} + (0.65)\Delta T_{\text{win}}, \quad (2)$$

where  $\Delta^{18}\text{O}_{\text{cell}}$  is also normalized to the AD 1941–1990 period. The term  $(-0.28)\Delta RH_{\text{grs}}$  accounts for signals from humidity-dependent  $^{18}\text{O}$ -enrichment of leaf waters during transpiration and is strongly analogous to RH-sensitive  $\Delta^{13}\text{C}$  dependence on stomatal conductance, as suggested by Verheyden et al. (2004),

while the term  $(0.65)\Delta T_{\text{win}}$  accounts for “Dansgaard” signals in the  $\delta^{18}\text{O}$  of snowmelt water used by the trees. Eq. (2) is consistent with evidence that relative humidity and temperature both exert first-order influence on the water-isotope labelling of cellulose under natural conditions (Burk and Stuiver, 1981; Yapp and Epstein, 1982; Edwards et al., 1985; Buhay and Edwards, 1995; Roden et al., 2000; Anderson et al., 2002; Sternberg et al., 2007).

Eqs. (1) and (2) can be solved to estimate past changes in relative humidity and temperature from pairs of cellulose  $\Delta^{13}\text{C}$  and  $\Delta^{18}\text{O}$  values in two ways, either by accounting only for first-order effects (i.e., ignoring the minor influence of  $\Delta T_{\text{grs}}$  on  $\Delta^{13}\text{C}$  analogous to the approach of Lipp et al., 1996) or by assuming that winter and growth season temperatures are likely to have varied in concert as climate evolved over the past millennium, i.e.,  $\Delta T_{\text{win}} \approx \Delta T_{\text{grs}}$ . Although the resulting differences in reconstructed  $\Delta RH_{\text{grs}}$  are very small (see below), we employed the latter approach, which is supported by general covariance between decadal-average winter and growth season temperatures in the Columbia Icefield area over the past century, including identical rising trends of +0.1 K/decade in grid-cell rehabilitated temperature data (CANGRID, 2000).

As shown in Figure 2, the derived  $\Delta RH_{\text{grs}}$  and  $\Delta T_{\text{win}}$  anomalies are subsequently expressed as z-scores to allow direct comparison of reconstructed patterns of variability with other proxy records. Because of the straightforward geometry of the response surfaces described by Eqs. (1) and (2), these patterns are strongly conservative over broad ranges of plausible variation in the four coefficients, providing the individual signs are conserved, although potential clearly exists to undertake more detailed calibration to support numerical estimation of  $\Delta RH_{\text{grs}}$  and  $\Delta T_{\text{win}}$  (see Buhay and Edwards, 1995; Roden et al., 2000; Anderson et al., 2002; McCarroll and Loader, 2004).

## Results

The raw composite decadal  $\delta^{13}\text{C}$  and  $\delta^{18}\text{O}$  dendrochronologies exhibit notably different patterns of variability over the past millennium (Fig. 2). The  $\delta^{13}\text{C}$  time series is marked by a progressive multicentennial oscillation of  $\sim 3$  ‰ amplitude about the “modern” AD 1941–90 mean, with generally low values in the early millennium, reaching a minimum around AD 1150 and high values in the late millennium, attaining a maximum around AD 1700, before declining to intermediate values in the 20th century. The companion  $\delta^{18}\text{O}$  record also fluctuates within a range of  $\sim 3$  ‰, albeit with substantially greater high-frequency variability, exhibiting three centennial-scale excursions above the 1941–90 mean in the 12th–14th, 16th and 18th–19th centuries.

We have developed two alternative scenarios from coupled modelling of the  $\delta^{13}\text{C}$  and  $\delta^{18}\text{O}$  dendrochronologies (Fig. 3). The “base-case” scenario (shown by dotted lines where it diverges from our favoured reconstruction) is derived from the configuration of the model indicated above, thus partitioning the isotope records into signals of changing source-water oxygen-isotope composition, transformed into equivalent winter temperature change ( $\Delta T_{\text{win}}$ ), and growth-season relative humidity ( $\Delta RH_{\text{grs}}$ ). As expected, reconstructed  $\Delta RH_{\text{grs}}$  is essentially an inversion of

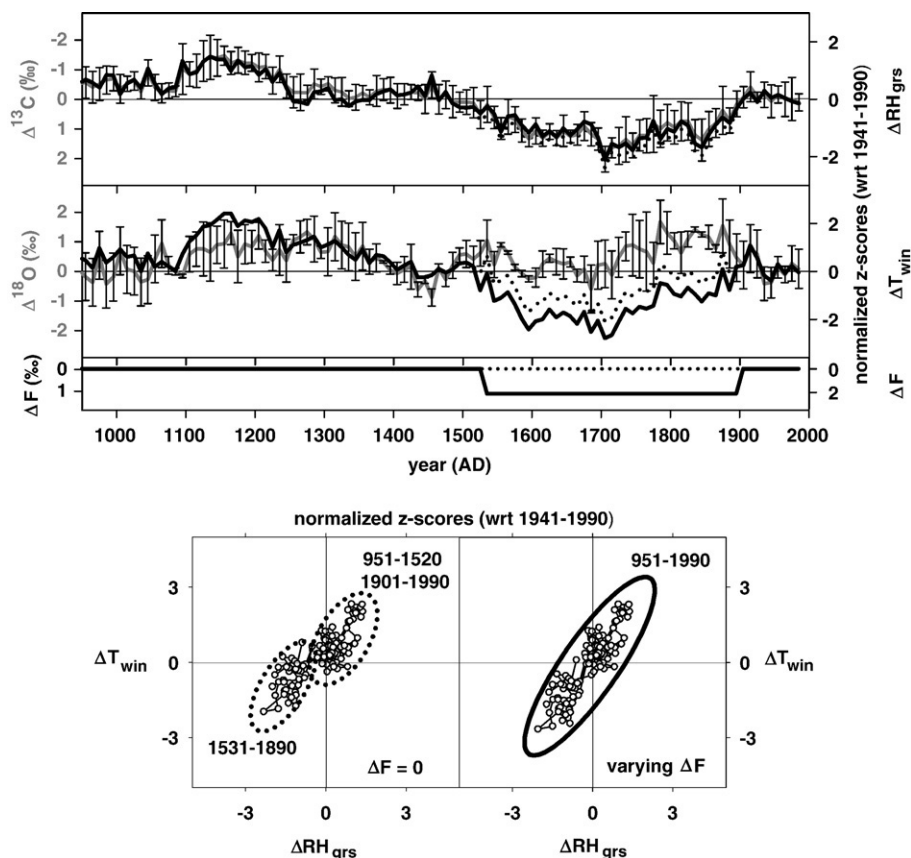


Figure 3. Reconstructed patterns of change in  $\Delta RH$  and  $\Delta T$  and the “Dansgaard offset” ( $\Delta F$ ), based on response–surface modelling of the  $\delta^{13}C$  and  $\delta^{18}O$  dendrochronologies in Figure 2. The isotope records (in grey) are shown for reference, expressed as  $\delta^{13}C$  and  $\delta^{18}O$  values normalized to the mean values of the AD 1941–1990 period, and with the  $\delta^{13}C$  record inverted to simplify comparison. The dotted and solid black lines indicate alternative reconstructions of  $\Delta RH_{grs}$  and  $\Delta T_{win}$  anomalies and prescribed  $\Delta F$ , as explained in the text. The solid black lines indicate our favoured reconstructions, incorporating a shift in  $\Delta F$  scaled to conserve low-frequency  $\Delta RH_{grs} - \Delta T_{win}$  stationarity, as shown in the crossplot at lower right and explained in the text. Note that the scale for  $\Delta F$  has also been inverted to enhance visual comparison with the other records.

the  $\delta^{13}C$  record, reflecting the predominating influence of stomatal conductance on carbon-isotope discrimination, while reconstructed  $\Delta T_{win}$  reflects separation of the  $\delta^{18}O$  record into  $\Delta T$ - and  $\Delta RH$ -dependent signals of similar magnitude.

Both reconstructions clearly display similar low-frequency oscillations, suggesting that early-millennium climate was marked by relatively warm winters and high growth season relative humidity, especially ~AD 1100–1250, followed by the onset of cooler and drier conditions in the early 1500s. Winter temperatures apparently attained 20th century levels by about AD 1800, while relatively low growth season humidity persisted until about AD 1900. The  $\Delta RH_{grs} - \Delta T_{win}$  crossplot shown at the lower left in Figure 3 reveals further intriguing details about this potential climate history. This includes a striking discontinuity in the pattern of inferred moisture–temperature variability over the period of record, with data grouped into two discrete linear clusters, such that the decades between the 1530s and 1890s are distinctly offset from the decades prior to and following this time interval. We can rule out the possibility that this feature is an artifact of analysis or compositing, since the transitions at the beginning and end of this episode occur within the lifespans of individual trees (and in multiple trees at two sites, in the early 1500s), although the apparent abruptness of the transitions is

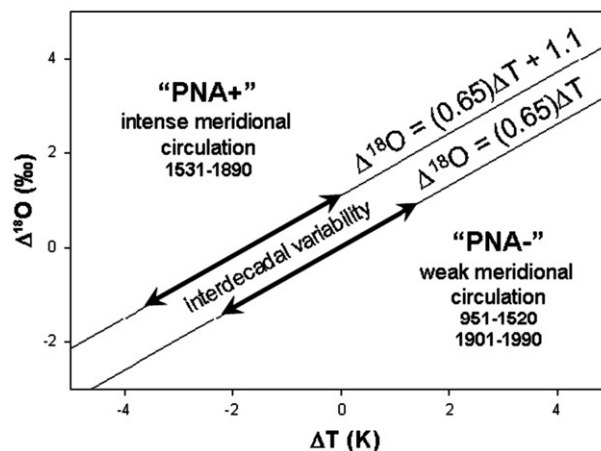


Figure 4. Schematic diagram showing the inferred offset ( $\Delta F$ ) in the “Dansgaard” precipitation  $\delta^{18}O - T$  relation in western Canada during the AD 1530s–1890s of +1.1‰ for the response–surface model as configured here. The offset is analogous to that associated with positive shifts in the Pacific–North American (PNA) index (Birks et al., 1998; Birks, 2003), which results in higher winter precipitation  $\delta^{18}O$  for a given temperature. Compare with Fricke and O’Neil (1999; Fig. 5) and Edwards et al. (1996; Fig. 3).

almost certainly exaggerated by the coarse temporal resolution of our data series.

On the other hand, we cannot preclude the possibility that this apparent non-stationarity in multicentennial moisture–temperature variability may instead be an artifact of the configuration of our response–surface model, which prescribes a constant “Dansgaard” isotope–temperature relation over the full span of our record, in spite of changes in climate. Hence, Figure 3 also shows a modified reconstruction that incorporates a small step-shift in this relation between the AD 1530s and 1890s that has the effect of conserving stationarity in moisture–temperature variability, while introducing (at a rudimentary level) an equivalent stationary oscillation in the “Dansgaard” relation. Notably, this fitted offset ( $\Delta F$ ; see Fig. 4) is consistent in both sense and magnitude with observed interannual variations in the precipitation isotope–temperature relation at stations in western Canada related to changes in the intensity of meridional circulation, as signified by variations in the Pacific–North American (PNA) index (Birks et al., 1998; Birks, 2003; see also data in Table 1 of Peng et al., 2004), as well as with circulation-dependent shifts in precipitation  $\delta^{18}\text{O}$  in the 19th century inferred from ice-core and lake-sediment records in southwestern Yukon (Fisher et al., 2004).

Although this simple adjustment of  $\Delta F$  certainly provides only a first-order approximation of the likely full pattern of variation in the local precipitation  $\delta^{18}\text{O}$ –temperature relation, conservation of stationarity in low-frequency moisture–temperature variability has the effect of very slightly reducing the inferred  $\Delta RH_{\text{grs}}$  anomaly (reflecting relatively weak temperature-dependence of cellulose  $\Delta^{13}\text{C}$ ) and more substantially deepening the  $\Delta T_{\text{win}}$  anomaly (reflecting relatively strong temperature-dependence of cellulose  $\Delta^{18}\text{O}$ ). While having little influence on the individual patterns of low-frequency moisture and temperature variability, this resolves the cool/dry conditions of the AD 1530s–1890s Little Ice Age interval into a singular climate episode, with both  $\Delta RH_{\text{grs}}$  and  $\Delta T_{\text{win}}$  returning to early 16th century levels by  $\sim$ AD 1900.

## Discussion

These isotope-based records combine with other paleodata to flesh out the chronicle of climatic and hydrologic changes over the past millennium in the eastern Rockies and neighbouring regions, compiled in Figure 5. The main components include characterization of variability in alpine climate, reflected in the

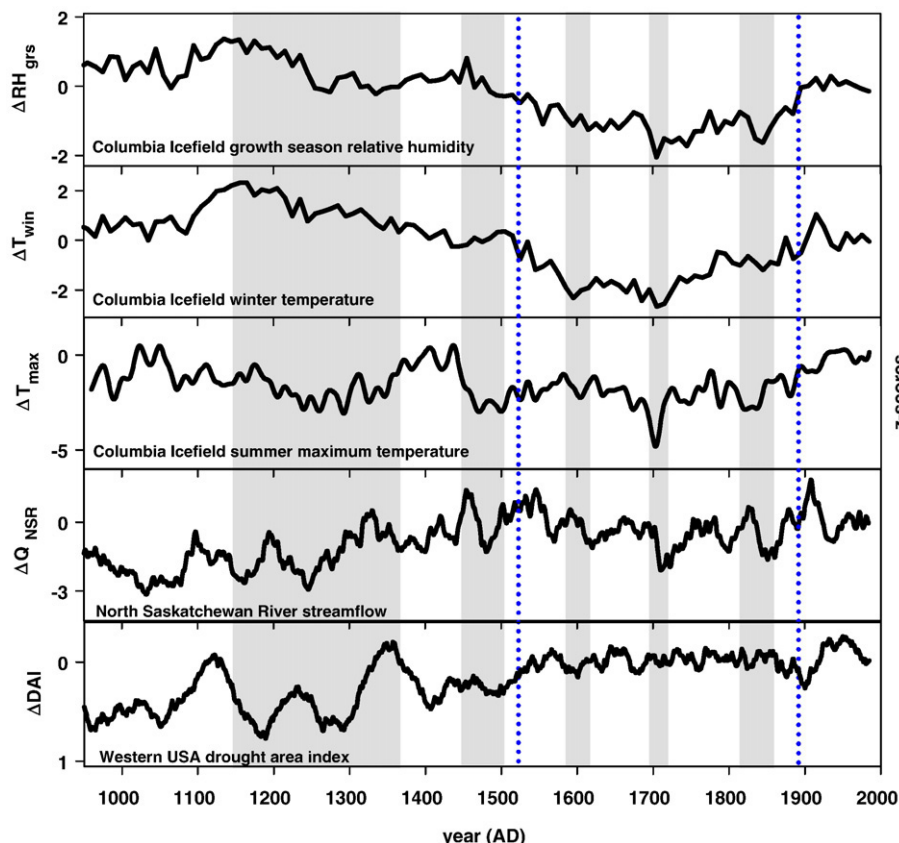


Figure 5. Compilation of isotope-based decadal  $\Delta RH_{\text{grs}}$  and  $\Delta T_{\text{win}}$  reconstructions with proxy climate and hydrologic time series from the eastern Rocky Mountains of western Canada and drought area index in the western USA. The dotted vertical lines indicate the timing of the step-shifts in the “Dansgaard” temporal precipitation  $\delta^{18}\text{O}$ –temperature relation prescribed to conserve stationarity in  $\Delta RH_{\text{grs}}-\Delta T_{\text{win}}$  variability (see Figs. 3 and 4). The shaded vertical bars depict approximate times of glacier expansion in the eastern Rockies, based on glaciologic and dendroglaciologic evidence and inference from suppression of summer temperature (Luckman, 1996, 2000; Osborn et al., 2001; Luckman and Villalba, 2001; see discussion in Luckman and Wilson, 2005). Maximum summer temperature ( $\Delta T_{\text{max}}$ ) is the RCS2004 reconstruction of Luckman and Wilson (2005), smoothed by a 20-yr moving cubic spline. North Saskatchewan River streamflow ( $\Delta Q_{\text{NSR}}$ ) is the Model 1 reconstruction of Case and MacDonald (2003) smoothed with a 20-yr moving average filter. Western USA drought area index ( $\Delta \text{DAI}$ ) reconstruction is from Cook et al. (2004), smoothed using a 60-yr moving window. Data from Cook et al. (2004) were obtained from the World Data Center for Paleoclimatology ([www.ncdc.noaa.gov/paleo/paleo.html](http://www.ncdc.noaa.gov/paleo/paleo.html)).

combination of varying summer relative humidity ( $\Delta RH_{\text{grs}}$ ), winter temperature ( $\Delta T_{\text{win}}$ ), and summer maximum temperature ( $\Delta T_{\text{max}}$ ); variability in runoff generation in rivers draining the eastern Rockies, represented by reconstructed North Saskatchewan River streamflow ( $\Delta Q_{\text{NSR}}$ ); and variability in regional glacial activity, shown by shaded bars depicting known or inferred times of glacier advance. Also included for comparison is the reconstruction of drought area index ( $\Delta \text{DAI}$ ) of Cook et al. (2004), which expresses contemporaneous hydrologic variability integrated over the neighbouring area of western USA.

The ~AD 1530s–1890s interval is marked by clear coherence among the  $\Delta RH_{\text{grs}}$ ,  $\Delta T_{\text{win}}$  and  $\Delta T_{\text{max}}$  reconstructions. All three records indicate the occurrence of cold and dry conditions in association with known advances of glaciers in the decades around AD 1700 and in the mid-1800s, plus a possible earlier episode ~AD 1600. Higher-frequency fluctuations also occur in  $\Delta Q_{\text{NSR}}$  at these times, perhaps reflecting corresponding shifts in icefield and glacier mass balance, superimposed upon generally higher streamflow than during preceding centuries, especially prior to ~AD 1350. The latter is in harmony with modern evidence that delayed snowmelt at times of colder temperatures tends to sustain higher streamflow in rivers draining the eastern slopes of the Rockies (Nkemdirim and Purves, 1994; Yulianti and Burn, 1998). This mechanism is additionally supported by results from paleoenvironmental studies in the Peace-Athabasca Delta, which lies downstream hydrologically and climatologically from the Columbia Icefield area, including paleolimnological evidence for elevated Lake Athabasca water levels between the mid-1500s and early 1900s attributable to elevated discharge at this time in the Athabasca River (Hall et al., 2004) and suppressed Peace River ice-jam flooding in the 18th and 19th centuries (Wolfe et al., 2006) likely linked to more prolonged seasonal snowmelt in the headwaters of the Smoky River (Prowse and Conly, 1998; Beltaos et al., 2006). Paleorecords from the Peace-Athabasca Delta also suggest the existence of dry atmospheric conditions in spite of higher river discharge, as indicated by intense desiccation in the early 1700s of perched lakes and wetlands isolated from the network of delta distributary channels (Wolfe et al., 2005).

Figure 5 also reveals that the ~AD 1530s–1890s interval corresponds closely in time with an extended period of persistently low reconstructed  $\Delta \text{DAI}$  in the adjoining western USA. An association with intensified meridional circulation and hence reduced influence from warm Pacific air masses in relation to cool Arctic air masses is suggested additionally by reconstructions of suppressed PDO variability at this time (MacDonald and Case, 2005) and negative NAO index (Cook, 2004), as well as by the large-scale spatial coherence, characteristic of positive PNA index under modern conditions (Jin et al., 2006). Positive PNA index, in turn, is strongly associated with a less vigorous circumpolar vortex, as manifested by negative Arctic Oscillation ( $\approx$ NAO) index (Quadrelli and Wallace, 2004).

The early millennium, in contrast, is characterized by a somewhat more complex history of climatic and hydrologic changes, as suggested by the differing patterns of variability among the

proxies illustrated in Figure 5. General correspondence is evident between mild climate at alpine treeline, indicated by elevated  $\Delta RH_{\text{grs}}$  and  $\Delta T_{\text{win}}$ , and hydrological drought downstream, indicated by low  $\Delta Q_{\text{NSR}}$ . This correspondence is especially clear prior to the early 1300s, which was marked by persistently high  $\Delta \text{DAI}$  in the western USA (Cook et al., 2004), suggesting that the annual snowpack commonly melted too quickly to adequately sustain streamflow and replenish soil moisture throughout a large area of western North America. High inferred winter temperatures ~AD 1100–1250 stand out in particular, corresponding with the Medieval Climate Anomaly and associated 12th century megadrought in western USA (MacDonald et al., 2008) and elevated temperatures in the Sierra Nevada (Millar et al., 2006). Substantial influence from the Pacific at this time is clearly signified by evidence for strong PDO variability (MacDonald and Case, 2005), while the large-scale spatial coherence is consistent with persistence of relatively weak meridional circulation, like that associated with negative PNA (Jin et al., 2006) and positive AO/NAO indices (Quadrelli and Wallace, 2004).

Other intriguing details are also apparent upon closer examination of the reconstructions. This includes divergence of the  $\Delta T_{\text{max}}$  record from the patterns of variability in  $\Delta RH_{\text{grs}}$  and  $\Delta T_{\text{win}}$  over two intervals, between the late 11th and late 14th centuries and in the 15th century, which contrasts with their general covariance during the later part of the record. Suppression of  $\Delta T_{\text{max}}$  over the earlier interval occurred in concert with glacier advances that began to override trees at Mount Robson beginning in the early 1100s (summarized by Luckman and Wilson, 2005), yet isotope-inferred  $\Delta RH_{\text{grs}}$  and  $\Delta T_{\text{win}}$  values suggest the onset of milder growing conditions around this time. Indeed, independent of model uncertainties, the lowest  $\delta^{13}\text{C}$  values of the entire millennial chronology, signifying especially strong discrimination against  $^{13}\text{C}$  and hence markedly favourable conditions for growth, occur in this interval in trees growing in the vicinities of both Athabasca and Bennington glaciers (and Robson Glacier pre-1150). This is consistent with the greater snowfall and cloudiness (and thus lower daytime temperatures and higher relative humidity) that are associated with negative PNA index under modern conditions in the mountains of western USA (Jin et al., 2006). The same mechanism can be invoked to explain low  $\Delta T_{\text{max}}$  in company with intermediate  $\Delta T_{\text{win}}$  and a slight rise in  $\Delta RH_{\text{grs}}$  during the possible subsequent advance of glaciers in the late 1400s indicated by evidence from minimum lichenometric ages on moraine fragments in Jasper National Park (Luckman, 2000). Changing icefield and glacier mass balance during the early millennium may also have contributed to higher-frequency fluctuations in the  $\Delta Q_{\text{NSR}}$  record suggested by the distinctive saw-tooth pattern of variability during the possible glacial advance of the late 1400s, reminiscent of variability during subsequent late-millennium episodes of glacier activity.

#### Summary and implications

Climate shifted broadly in western Canada from warm in winter and atmospherically moist during the growth season

during medieval times to being cool in winter and atmospherically dry during the growth season in the subsequent Little Ice Age, prior to the 20th century. This low-frequency climate oscillation was driven by systematic changes in the intensity of meridional circulation, manifested by variations in the relative influence of warm/moist Pacific and cold/dry Arctic air masses in the region and attendant changes in the precipitation  $\delta^{18}\text{O}$ –temperature relation, analogous to climate dynamics associated with fluctuations in the PNA index at interannual time-scales. Glacier advances occurred under both regimes, driven by increased snowfall at high elevations at times of intensified zonal circulation during the early millennium and by decreased temperature at times of intensified meridional circulation during the LIA. Streamflow variability in rivers draining the eastern Rockies responded strongly to changes in the timing of annual snowmelt.

Hydrological drought during medieval times evidently influenced a vast area of western North America, propagating across the northern Great Plains of western Canada into the upper reaches of both the Saskatchewan and Mackenzie river systems, two major sources of freshwater runoff to the arctic. Declining streamflow in rivers draining the eastern Rockies over the past century (Rood et al., 2005) may indicate that conditions are in the process of returning to a similar state, with potentially serious consequences given escalating industrial, agricultural and municipal demands on water resources in this region (Schindler and Donahue, 2006; Schindler and Smol, 2006).

## Acknowledgments

This research was supported by the Natural Sciences and Engineering Research Council of Canada, the British Columbia Hydro and Power Authority, and the National Science Foundation (USA). The insightful comments of two reviewers and the Associate Editor (D.J. Meltzer) were greatly appreciated.

## References

- Amundsen, R., Chadwick, O., Kendall, C., Wang, Y., DeNiro, M., 1996. Isotopic evidence for shifts in atmospheric circulation patterns during the late Quaternary in mid-North America. *Geology* 24, 23–26.
- Anderson, W.T., Bernasconi, S.M., McKenzie, J.A., Saurer, M., Schweingruber, F., 2002. Model evaluation for reconstructing the oxygen isotopic composition in precipitation from tree ring cellulose over the last century. *Chemical Geology* 182, 121–137.
- Bartlein, P.J., Webb III, T., Fleri, E., 1984. Holocene climatic change in the northern Midwest: Pollen derived estimates. *Quaternary Research* 22, 361–374.
- Beltaos, S., Prowse, T.D., Bonsal, B.R., MacKay, R., Romolo, L., Pietroniro, A., Toth, B., 2006. Climatic effects on ice-jam flooding in the Peace-Athabasca Delta. *Hydrological Processes* 20, 4031–4050.
- Birks, S.J., 2003. Water isotope partitioning in aquitards and precipitation on the Northern Great Plains. Ph.D. Thesis, University of Waterloo, Ontario, Canada, 291 pp.
- Birks, S.J., Edwards, T.W.D., Remenda, V.H., 1998. Synoptic climatological analysis of IAEA/WMO GNIP data from Canada: possible evidence for ENSO influence on isotope-climate relations. *Proceedings, Isotope Techniques in the Study of Environmental Change*, Vienna, April 1997, IAEA-SM-349/4P, pp. 767–770.
- Bradley, R.S., Briffa, K.R., Cole, J., Hughes, M.K., Osborn, T.J., 2003. The climate of the last millennium. In: Alverson, K.D., Bradley, R.S., Pederson, T.F. (Eds.), *Paleoclimate, Global Change and the Future*. Springer-Verlag, Berlin, pp. 105–142.
- Bryson, R., Wendland, W., 1967. Tentative climatic patterns for some late-glacial and postglacial episodes in central North America. In: Dort Jr., W., Jones Jr., J.K. (Eds.), *Pleistocene and recent environments of the Central Great Plains*. University of Manitoba Press, Winnipeg, pp. 271–298.
- Buhay, W.M., Edwards, T.W.D., 1995. Climate in southwestern Ontario, Canada, between AD 1610 and 1885 inferred from oxygen and hydrogen isotopic measurements of wood cellulose from trees in different hydrologic settings. *Quaternary Research* 44, 438–446.
- Burk, R.L., Stuiver, M., 1981. Oxygen isotope ratios in trees reflect mean annual temperature and humidity. *Science* 211, 1417–1419.
- CANGRID, 2000. Monthly rehabilitated gridded Canadian historical air temperature and precipitation database. Climate Research Branch, Meteorological Service of Canada, Toronto (CD-ROM).
- Case, R.A., MacDonald, G.M., 2003. Tree ring reconstructions of streamflow for three Canadian Prairie Rivers. *Journal of the American Water Resources Association* 39, 703–716.
- Clague, J.J., Mathewes, R.W., Buhay, W.M., Edwards, T.W.D., 1992. Early Holocene climate at Castle Peak, southern Coast Mountains, British Columbia, Canada. *Palaeogeography, Palaeoclimatology, Palaeoecology* 95, 153–167.
- Cook, E.R., 2004. Multi-Proxy Reconstructions of the North Atlantic Oscillation (NAO) Index: a critical review and a new well-verified winter NAO index reconstruction back to AD 1400. In: Hurrell, J.W., Kushnir, Y., Ottersen, G., Visbeck, M. (Eds.), *The North Atlantic Oscillation: Climate Significance and Environmental Impact*. American Geophysical Union, Washington DC. doi:10.1029/134GM04. Geophysical Monograph 134.
- Cook, E.R., Woodhouse, C.A., Eakin, C.M., Meko, D.M., Stahle, D.W., 2004. Long-term aridity changes in the western United States. *Science* 306, 1015–1018.
- Cook, E.R., Seager, R., Cane, M.A., Stahle, D.W., 2007. North American drought: Reconstructions, causes, and consequences. *Earth-Science Reviews* 81, 93–134.
- Coplen, T.B., 1996. New guidelines for reporting stable hydrogen, carbon and oxygen isotope-ratio data. *Geochimica et Cosmochimica Acta* 60, 3359–3360.
- Crowley, T.J., Lowery, T.S., 2000. How warm was the Medieval Warm Period? *Ambio* 29, 51–54.
- D'Arrigo, R., Wilson, R., Jacoby, G., 2006. On the long-term context for late twentieth century warming. *Journal of Geophysical Research* 111, D03103. doi:10.1029/2005JD006352.
- Danis, P.A., Masson-Delmotte, V., Stievenard, M., Guillemin, M.T., Daux, V., Naveau, Ph., von Grafenstein, U., 2006. Reconstruction of past precipitation  $\delta^{18}\text{O}$  using tree-ring cellulose  $\delta^{18}\text{O}$  and  $\delta^{13}\text{C}$ : a calibration study near Lac d'Annecy, France. *Earth and Planetary Science Letters* 243, 439–448.
- Dansgaard, W., 1964. Stable isotopes in precipitation. *Tellus* 16, 436–468.
- Edwards, T.W.D., Aravena, R.O., Fritz, P., Morgan, A.V., 1985. Interpreting paleoclimate from  $^{18}\text{O}$  and  $^2\text{H}$  in plant cellulose: comparison with evidence from fossil insects and relict permafrost in southwestern Ontario. *Canadian Journal of Earth Sciences* 22, 1720–1726.
- Edwards, T.W.D., Fritz, P., 1986. Assessing meteoric water composition and relative humidity from  $^{18}\text{O}$  and  $^2\text{H}$  in wood cellulose: paleoclimatic implications for southern Ontario, Canada. *Applied Geochemistry* 1, 715–723.
- Edwards, T.W.D., Luckman, B.H., 1996. Isotope dendroclimatology studies in the Canadian Rockies: some preliminary results. In: Dean, J.S., Meko, D.M., Swetnam, T.W. (Eds.), *Tree Rings, Environment and Humanity*. Radiocarbon, 38, pp. 585–596.
- Edwards, T.W.D., Wolfe, B.B., MacDonald, G.M., 1996. Influence of changing atmospheric circulation on precipitation  $\delta^{18}\text{O}$ -temperature relations in Canada during the Holocene. *Quaternary Research* 46, 211–218.
- Edwards, T.W.D., Graf, W., Trimbom, P., Stichler, W., Lipp, J., Payer, H.D., 2000.  $\delta^{13}\text{C}$  response surface resolves humidity and temperature signals in trees. *Geochimica et Cosmochimica Acta* 64, 161–167.
- Esper, J., Cook, E.R., Schweingruber, F.H., 2002. Low-frequency signals in long tree-ring chronologies for reconstructing past temperature variability. *Science* 295, 2250–2253.
- Esper, J., Frank, D.C., Wilson, R.J.S., Briffa, K.R., 2005a. Effect of scaling and regression on reconstructed temperature amplitude for the past millennium. *Geophysical Research Letters* 32, L07711. doi:10.1029/2004GK021236.

- Esper, J., Wilson, R.J.S., Frank, D.C., Moberg, A., Wanner, H., Luterbacher, J., 2005b. Climate: past ranges and future changes. *Quaternary Science Reviews* 24, 2164–2166.
- Farquhar, G.D., O'Leary, M.H., Berry, J.A., 1982. On the relationship between carbon isotope discrimination and the intercellular carbon dioxide concentration of leaves. *Australian Journal of Plant Physiology* 9, 121–137.
- Fisher, D.A., Wake, C., Kreutz, K., Yalcin, K., Steig, E., Mayewski, P., Anderson, L., Zheng, J., Rupper, S., Zdanowicz, C., Demuth, M., Waszkiewicz, M., Dahl-Jensen, N.D., Goto-Azuma, K., Bourgeois, J.B., Koerner, R.M., Sekerka, J., Osterberg, E., Abbott, M.B., Finney, B.P., Burns, S.J., 2004. Stable isotope records from Mount Logan, Eclipse ice cores and nearby Jellybean Lake. Water cycle of the North Pacific over 2000 years and over five vertical kilometres: sudden shifts and tropical connections. *Géographie physique et Quaternaire* 58, 337–352.
- Folland, C.K., Karl, T.R., Christy, J.R., Clarke, R.A., Gruza, G.V., Jouzel, J., Mann, M.E., Oerlemans, J., Salinger, M.J., Wang, S.-W., 2001. Observed climate variability and change. In: Houghton, J.T., Ding, Y., Griggs, D.J., Noguer, M., van der Linden, P.J., Xiaosu, D. (Eds.), *Climate Change 2001: The Scientific Basis*. Cambridge University Press, New York, pp. 99–181.
- Fricke, H.C., O'Neil, J.R., 1999. The correlation between  $^{18}\text{O}/^{16}\text{O}$  ratios of meteoric water and surface temperature: its use in investigating terrestrial climate change over geologic time. *Earth and Planetary Science Letters* 170, 181–196.
- Hall, R.I., Wolfe, B.B., Edwards, T.W.D., 2004. A Multi-Century Flood, Climatic, and Ecological History of the Peace-Athabasca Delta, Northern Alberta, Canada. Final Report. Published by BC Hydro, 163 pp. + Appendices.
- Hammarlund, D., Barnekow, L., Birks, H.J.B., Buchardt, B., Edwards, T.W.D., 2002. Holocene changes in atmospheric circulation recorded in the oxygen-isotope stratigraphy of lacustrine carbonates from northern Scandinavia. *The Holocene* 12, 339–351.
- Hammarlund, D., Velle, G., Wolfe, B.B., Edwards, T.W.D., Snowball, I., Barnekow, L., Holmgren, S., Lamme, S., Wohlfarth, B., Possnert, G., 2004. Palaeolimnological and sedimentary responses to Holocene forest retreat in the Scandes Mountains, west-central Sweden. *The Holocene* 14, 862–876.
- Herweijer, C., Seager, R., Cook, E.R., 2006. North American droughts of the mid to late nineteenth century: a history, simulation and implication for Mediaeval drought. *The Holocene* 16, 159–171.
- Hoffmann, G., Jouzel, J., Johnsen, S., 2001. The deuterium excess record from central Greenland over the last millennium: hints of a North Atlantic signal during the Little Ice Age. *Journal of Geophysical Research* 106, 14, 265–14,274.
- Jin, J., Norman, N.L., Sorooshian, S., Gao, X., 2006. Relationship between atmospheric circulation and snowpack in the western USA. *Hydrological Processes* 20, 753–767.
- Kirby, M.E., Mullins, H.T., Patterson, W.P., Burnett, A.W., 2001. Lacustrine isotopic evidence for multidecadal natural climate variability related to the circumpolar vortex over northeast United States during the past millennium. *Geology* 29, 807–810.
- Kreutz, K.J., Mayewski, P.A., Meecker, L.D., Twickler, M.S., Whitlow, S.I., Pittalwala, I.I., 1997. Bipolar changes in atmospheric circulation during the Little Ice Age. *Science* 277, 1294–1296.
- Lamb, H.H., 1977. *Climate History and the Future*, vol. 2, Climate: Present, Past, and Future. Methuen, New York, 835 pp.
- Leavitt, S.W., Panyushkina, I.P., Lange, T., Wiedenhoeft, A., Cheng, L., Hunter, R.H., Hughes, J., Pranschke, F., Schneider, A.L., Moran, J., Stieglitz, R., 2006. Climate in the Great Lakes region between 14,000 and 4000 years ago from isotopic composition of conifer wood. *Radiocarbon* 48, 205–217.
- Lipp, J., Trimbom, P., Edwards, T.W.D., Waisel, Y., Yakir, D., 1996. Climatic effects on the  $\text{d}^{18}\text{O}$  and  $\text{d}^{13}\text{C}$  of cellulose in the desert tree *Tamarix jordanis*. *Geochimica et Cosmochimica Acta* 60, 3305–3309.
- Luckman, B.H., 1996. Dendroglaciology at Peyto Glacier, Alberta. In: Dean, J.S., Meko, D.M., Swetnam, T.W. (Eds.), *Tree Rings, Environment and Humanity*. Radiocarbon, 38, pp. 679–688.
- Luckman, B.H., 2000. The Little Ice Age in the Canadian Rockies. *Geomorphology* 32, 357–384.
- Luckman, B.H., Villalba, R., 2001. Assessing synchronicity of glacier fluctuations in the western cordillera of the Americas during the last millennium. In: Markgraf, V. (Ed.), *Interhemispheric Climate Linkages*. Academic Publishers, San Diego, pp. 119–140.
- Luckman, B.H., Wilson, R.J.S., 2005. Summer temperatures in the Canadian Rockies during the last millennium: a revised record. *Climate Dynamics* 24, 131–144.
- MacDonald, G.M., Case, R.A., 2005. Variations in the Pacific Decadal Oscillation over the past millennium. *Geophysical Research Letters* 32, L08703. doi:10.1029/2005GL022478.
- MacDonald, G.M., Velichko, A.A., Kremenetski, C.V., Borisova, O.K., Goleva, A.A., Andreev, A.A., Cwynar, L.C., Riding, R.T., Forman, S.L., Edwards, T.W.D., Aravena, R., Hammarlund, D., Szeicz, J.M., Gattaulin, V.N., 2000. Holocene treeline history and climate change across northern Eurasia. *Quaternary Research* 53, 302–311.
- MacDonald, G.M., Kremenetski, K.V., Hidalgo, H.G., 2007. Southern California and the perfect drought: Simultaneous prolonged drought in southern California and the Sacramento and Colorado river systems. *Quaternary International*. doi:10.1016/j.quaint.2007.06.027.
- MacDonald, G.M., Stahle, D.W., Diaz, J.V., Beer, N., Busby, S.J., Cerano-Peredes, J., Cole, J.E., Cook, E.R., Endfield, G., Gutierrez-Garcia, G., Hall, B., Magana, V., Meko, D.M., Méndez-Pérez, M., Sauchyn, D.J., Watson, E., Woodhouse, C., 2008. Climate warming and 21st-century drought in southwestern North America. *EOS* 89, 82.
- Mann, M.E., Bradley, R.S., Hughes, M.K., 1999. Northern Hemisphere temperatures during the last millennium: inferences, uncertainties and limitations. *Geophysical Research Letters* 26, 759–762.
- Mann, M.E., Rutherford, S., Wahl, E., Ammann, C., 2005. Testing the fidelity of methods used in proxy-based reconstructions of past climate. *Journal of Climate* 18, 4097–4107.
- Mayr, C., Trimbom, P., Lipp, J., Grams, T.E.E., Graf, W., Payer, H.D., Stichler, W., 2004. Climate information from stable hydrogen and carbon isotopes of C3 plants — growth chamber experiments and field observations. In: Fischer, H., Kumke, T., Lohmann, G., Flöser, G., Miller, H., von Storch, H., Negendank, J.F.W. (Eds.), *The Climate in Historical Times — Towards a Synthesis of Holocene Proxy Data and Climate Models*. Springer Verlag, Berlin, pp. 263–279.
- McCarroll, D., Loader, N.J., 2004. Stable isotopes in tree rings. *Quaternary Science Reviews* 23, 771–801.
- McKenzie, J.A., Hollander, D., 1993. Oxygen-isotope record in recent carbonate sediments from Lake Greifen, Switzerland (1750–1986): Application of continental isotopic indicator for evaluation of changes in climate and atmospheric circulation patterns. In: Swart, P.K., McKenzie, J., Lohmann, K.C., Savin, S. (Eds.), *Climate Change in Continental Isotopic Records*. Geophysical Monograph, 78. American Geophysical Union, Washington DC, pp. 101–111.
- Meko, D.M., Therrell, M.D., Baisan, C.H., Hughes, M.K., 2001. Sacramento River flow reconstructed to A.D. 869 from tree rings. *Journal of the American Water Resources Association* 37, 1029–1039.
- Millar, C.I., King, J.C., Westfall, R.D., Alden, H.A., Delany, D.L., 2006. Late Holocene forest dynamics, volcanism, and climate change at Whiting Mountain and San Joachim Ridge, Mono County, Sierra Nevada, CA, USA. *Quaternary Research* 66, 273–287.
- Moberg, A., Sonechkin, D.N., Holmgren, K., Datsenko, N.M., Karlén, W., 2005. Highly variable Northern Hemisphere temperatures reconstructed from low- and high-resolution proxy data. *Nature* 433, 613–617.
- Nkemdirim, L.C., Purves, H., 1994. Estimating the potential impact of climate change on streamflow in the Oldman River basin, Alberta: an analogue approach. *Canadian Water Resources Journal* 19, 185–200.
- Osborn, G.D., Robinson, B.J., Luckman, B.H., 2001. Holocene and latest Pleistocene fluctuations of Stutfield Glacier, Canadian Rockies. *Canadian Journal of Earth Sciences* 38, 1141–1155.
- Pendall, E., Betancourt, J.L., Leavitt, S.W., 1999. Paleoclimatic significance of  $\delta^2\text{H}$  and  $\delta^{13}\text{C}$  values in piñon pine needles from packrat middens spanning the last 40,000 years. *Palaeogeography, Palaeoclimatology, Palaeoecology*, 147, 53–72.
- Peng, H., Mayer, B., Harris, S., Krouse, H.R., 2004. A 10-yr record of stable isotope ratios of hydrogen and oxygen in precipitation at Calgary, Alberta, Canada. *Tellus* 56B, 147–159.
- Plummer, L.N., 1993. Stable isotope enrichment in paleowaters of the southeast Atlantic coastal plain, United States. *Science* 262, 2016–2020.
- Prowse, T.D., Conly, F.M., 1998. Effects of climatic variability and flow regulation on ice-jam flooding of a northern delta. *Hydrological Processes* 12, 1589–1610.

- Quadrelli, R., Wallace, J.M., 2004. A simplified linear framework for interpreting patterns of Northern Hemisphere wintertime climate variability. *Journal of Climate* 17, 3728–3744.
- Ramirez, E., Hoffmann, G., Taupin, J.D., Francou, B., Ribstein, P., Caillon, N., Ferron, F.A., Landais, A., Petit, J.R., Pouyaud, B., Schotterer, U., Simoes, J.C., Stievenard, M., 2003. A new Andean deep ice core from Nevado Illimani (6350 m), Bolivia. *Earth and Planetary Science Letters* 212, 337–350.
- Roden, J.S., Lin, G., Ehleringer, J.R., 2000. A mechanistic model for interpretation of hydrogen and oxygen isotope ratios in tree-ring cellulose. *Geochimica et Cosmochimica Acta* 64, 21–35.
- Rood, S.B., Samuelson, G.M., Weber, J.K., Wyrot, K.A., 2005. Twentieth-century decline in streamflows from the hydrographic apex of North America. *Journal of Hydrology*, 306, 215–233.
- Scheidegger, Y., Saurer, M., Bahn, M., Siegwolf, R., 2000. Linking stable oxygen and carbon isotopes with stomatal conductance and photosynthetic capacity: a conceptual model. *Oecologia* 125, 350–357.
- Schindler, D.W., Donahue, W.F., 2006. An impending water crisis in Canada's western prairie provinces. *PNAS* 103, 7210–7216.
- Schindler, D.W., Smol, J.P., 2006. Cumulative effects of climate warming and other human activities on freshwaters of arctic and subarctic North America. *Ambio* 35, 160–168.
- Sternberg, L.S.L., 1989. Oxygen and hydrogen isotope measurements in plant cellulose analysis. In: Linskens, H.F., Jackson, J.F. (Eds.), *Plant Fibers*. Springer-Verlag, New York, pp. 89–99.
- Sternberg, L.S.L., Pinzon, M.C., Vendramini, P.F., Anderson, W.T., Jahren, A.H., Beuning, K., 2007. Oxygen isotope ratios of cellulose-derived phenylglucosaminose: An improved paleoclimate indicator of environmental water and relative humidity. *Geochimica et Cosmochimica Acta* 71, 2463–2473.
- Treydte, K.S., Schleser, G.H., Helle, G., Frank, D.C., Winiger, M., Haug, G.H., Esper, J., 2006. The twentieth century was the wettest period in northern Pakistan over the past millennium. *Nature* 440, 1179–1182.
- Verheyden, A., Helle, G., Schleser, G.H., Dehairs, F., Beeckman, H., Koedam, N., 2004. Annual cyclicality in high-resolution stable carbon and oxygen isotope ratios in the wood of the mangrove tree *Rhizophora mucronata*. *Plant, Cell and Environment* 27, 1525–1536.
- von Storch, H., Zorita, E., Jones, J.M., Dimitriev, Y., González-Rouco, F., Tett, S.F.B., 2004. Reconstructing past climate from noisy data. *Science* 306, 679–682.
- Watson, E., Luckman, B.H., 2001. Dendroclimatic reconstruction of precipitation for sites in the southern Canadian Rockies. *The Holocene* 11, 203–213.
- Watson, E., Luckman, B.H., 2004. Tree-ring-based mass-balance estimates for the last 300 years at Peyto Glacier, Alberta, Canada. *Quaternary Research* 62, 9–18.
- Watson, E., Luckman, B.H., 2005. An exploration of the controls of pre-instrumental streamflow using multiple tree-ring proxies. *Dendrochronologia* 22, 225–234.
- Watson, E., Luckman, B.H., 2006. Long hydroclimate records from tree-rings in western Canada: potential, problems and prospects. *Canadian Water Resources Journal* 31, 1–24.
- Wolfe, B.B., Karst-Riddoch, T.L., Vardy, S.R., Falcone, M.D., Hall, R.I., Edwards, T.W.D., 2005. Impacts of climate and river flooding on the hydroecology of a floodplain basin, Peace-Athabasca Delta, Canada since AD 1700. *Quaternary Research* 64, 147–162.
- Wolfe, B.B., Hall, R.I., Last, W.M., Edwards, T.W.D., English, M.C., Karst-Riddoch, T.L., Paterson, A., Palmini, R., 2006. Reconstruction of multi-century flood histories from oxbow lake sediments, Peace-Athabasca Delta, Canada. *Hydrological Processes*, 20. doi:10.1002/hyp.6423.
- Yakir, D., Gat, J., Issar, A., Adar, E., Trimborn, P., Lipp, J., 1994.  $^{13}\text{C}$  and  $^{18}\text{O}$  of wood from the Roman siege rampart in Masada (AD 70–73): evidence for a less arid climate for the region. *Geochimica et Cosmochimica Acta* 58, 3535–3539.
- Yapp, C.R., Epstein, S., 1977. Climatic implications of D/H ratios of meteoric waters over North America (9500–22,000 BP) as inferred from ancient wood cellulose C-H hydrogen. *Earth and Planetary Science Letters* 34, 333–350.
- Yapp, C.R., Epstein, S., 1982. A re-examination of cellulose carbon-bound hydrogen  $\delta\text{D}$  measurements and some factors affecting plant-water D/H relationships. *Geochimica et Cosmochimica Acta* 46, 955–965.
- Yulianti, J., Burn, D., 1998. Investigating links between climate warming and low streamflow in the prairie region of Canada. *Canadian Water Resources Journal* 23, 45–60.